Immunology research using ImageStream Cytometry

The ImageStream system combines high-speed image capture with image quantification to create a statistically powerful microscopy platform, enabling robust discrimination of cells based on their appearance. This document highlights applications of ImageStream cytometry to the field of immunology as described in publications, posters and podium presentations. For more information, check out the website: (https://www.amnis.com/immunology.html)

Table of Contents:

Endosomal trafficking of SLE immune complexes in human monocytes 2

Quantification of receptor recruitment to the immune synapse 2-3

Inhibition of T cell-dendritic cell conjugate formation by Treg cells 3

Clustering of LFA as a measure of T cell activation 4

Preferential pDC-MDCC conjugate formation and transfer of cellular components with HSV infection 4

Expression and maintenance of KHSV infection in tonsillar B cells 5

HIV-induced nuclear translocation of IRF3 5

Measurement of TLR-mediated NF-κB nuclear translocation in whole blood pDC 6

Internalization of exosomes by monocytes 6

Merocytosis of irradiated β-islet cell fragments by mcDCs 7

c-Myc-induced apoptosis of terminally differentiating B cells 7

Reference List 8-10

Endosomal trafficking of SLE immune complexes in human monocytes

Summary: This ImageStream assay quantifies the C1q-induced subcellular trafficking of systemic lupus erythematosis (SLE) immune complexes (IC) within human monocytes. The ImageStream's high speed imaging capacity enabled analysis of 10,000 events per sample for robust statistics. The co-localization feature used (bright detail similarity) measures the pixel-by-pixel correlation between the SLE IC and CD71 (or LAMP-1) images.

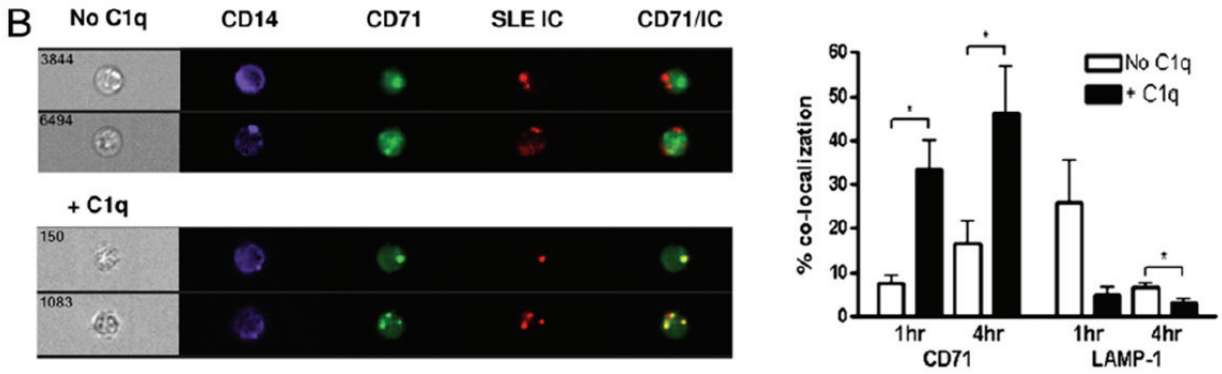

"Our study provides novel evidence to explain how C1q blocks IFN-α production. It demonstrates that C1q enhances the binding of ICs to both monocytes and pDCs. When monocytes were absent, C1q augmented IC binding to pDCs and led to increased IFN-α production. However, when monocytes were present, C1q preferentially and almost exclusively promoted the uptake of ICs by these cells, leading to accumulation in early endosomes and decreased IFN-α production by pDCs."

Reference: Santer, D.M., B.E. Hall, T.C. George, S. Tangsombatvisit, C.L. Liu, P.D. Arkwright, and K.B. Elkon, *C1q deficiency leads to the defective suppression of IFN-alpha in response to nucleoprotein containing immune complexes.* J Immunol, 2010. **185**(8): 4738-49.

~ ~ ~ ~ ~ ~

Quantification of receptor recruitment to the immune synapse

Summary: This ImageStream assay quantifies the accumulation of CD3/LFA-1 (B, C; left plots) or F-actin (B, C; right plots) at the immune synapse (IS) between B-T conjugates. The ImageStream's high speed imaging capacity enabled analysis of 20,000 events per sample for robust statistics. The feature used (Fold increase) is the ratio of the mean pixel intensity (MPI) at the contact zone to the MPI within the T cell. Representative conjugates are shown in (A).

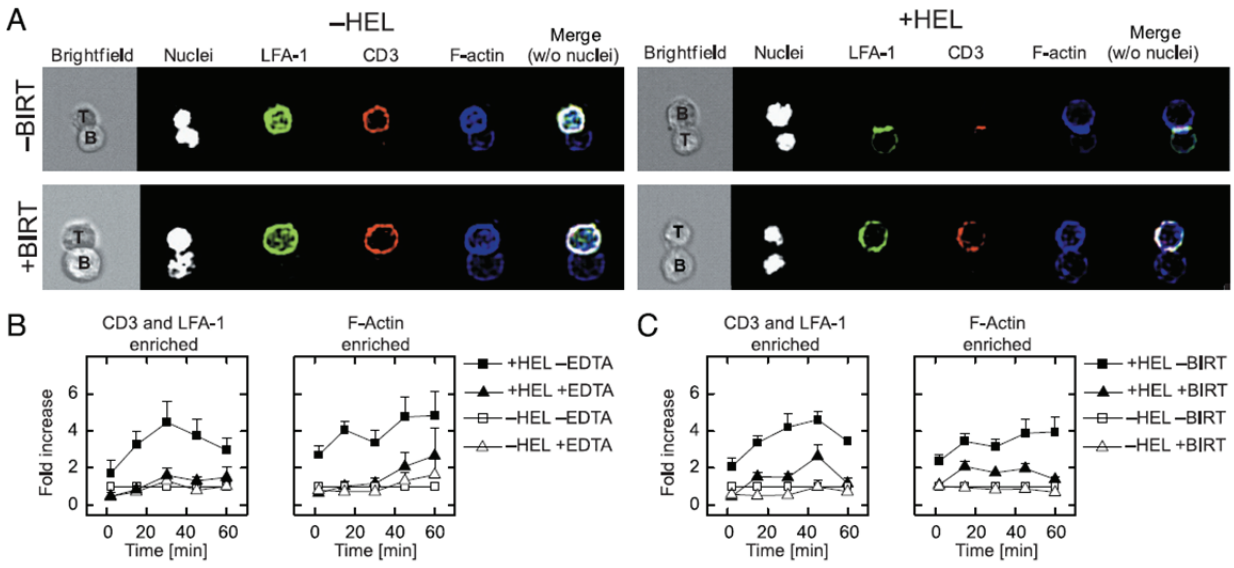

"To study the kinetics of receptor accumulation and IS maturation at the contact zone of 3B11 T cells and LK35.2 B cells, all cell couples were analyzed by multispectral imaging flow cytometry (MIFC), using the Image Stream system. MIFC is a method that combines the advantages of a high-throughput flow cytometer and fluorescence microscopy (19), thereby allowing rapid quantitative and objective analysis of proteins in the contact zone between T cells and APCs for all T-cell/APC pairs within a given population.."

Reference: Hosseini, B.H., I. Louban, D. Djandji, G.H. Wabnitz, J. Deeg, N. Bulbuc, Y. Samstag, M. Gunzer*, et al.*, *Immune synapse formation determines interaction forces between T cells and antigen-presenting cells measured by atomic force microscopy.* Proc Natl Acad Sci U S A, 2009. **106**(42): 17852-7.

Related reference from the same group: Hoffman 2011 Hoffmann, S., B.H. Hosseini, M. Hecker, I. Louban, N. Bulbuc, N. Garbi, G.H. Wabnitz, Y. Samstag*, et al.*, *Single cell force spectroscopy of T cells recognizing a myelin-derived peptide on antigen presenting cells.* Immunol Lett, 2011. **136**(1): 13-20.

~ ~ ~ ~ ~ ~

Inhibition of Tcell-dendritic cell conjugate formation by Treg cells

Summary: This ImageStream assay quantifies conjugate formation between conventional T cells (Tcon, red) and DC (blue) in the presence of regulatory T cells (Treg, green). The ImageStream's high speed imaging capacity enabled analysis of thousands of events per sample for robust statistics. As shown in the table at right, a higher percentage of Treg-containing conjugates from mice with deficient SHP-1 (motheaten (me)) were co-conjugated with Tcons. Further ImageStream studies go on to show that Tcons conjugated to APCs with Tregs are not activated as evidenced by an almost complete failure to upregulate CD25 or express IL-2.

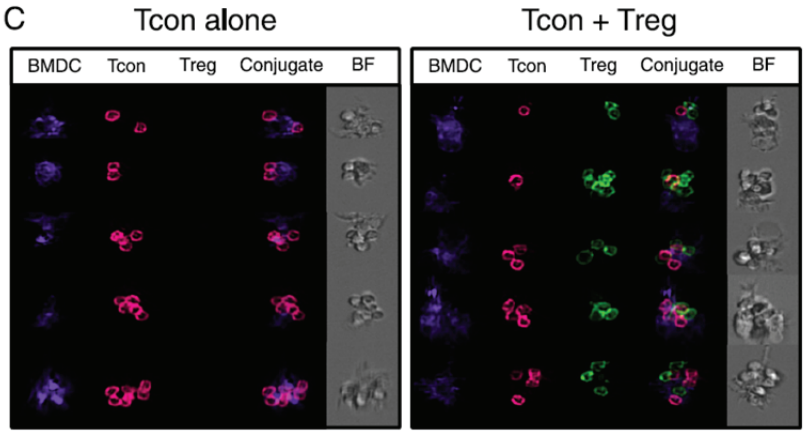

% of Treg-containing conjugates within Tcon/BMDC conjugates	100 ng OVA peptide	500 ng OVA peptide
Tcon *alone*	—	—
Tcon plus Treg (+/+)	30 %	47 %
Tcon plus Treg (*me*/+)	40 %	54 %
Tcon plus Treg (*me/me*)	52 %	67 %

"Finally, through a quantitative imaging approach, we directly demonstrate that Tregs prevent the activation of Tcon and that SHP-1–deficient Tregs are more efficient suppressors. Collectively, our data reveal SHP-1 as a critical modifier of Treg function and a potential therapeutic target for augmenting Treg-mediated suppression in certain disease states."

Reference: Iype, T., M. Sankarshanan, I.S. Mauldin, D.W. Mullins, and U. Lorenz, *The protein tyrosine phosphatase SHP-1 modulates the suppressive activity of regulatory T cells.* J Immunol, 2010. **185**(10): 6115-27.

Clustering of LFA as a measure of T cell activation

Summary: This ImageStream assay quantifies HTMT-induced inhibition of LFA-1 polarization in specific peptide-activated T cells. Cells with uniform, clustered or capped LFA distributions were distinguished from each other using threshold area (clusters and caps have low values) and delta centroid (polarized tendency of a stain, caps have high values) metrics present in the IDEAS software.

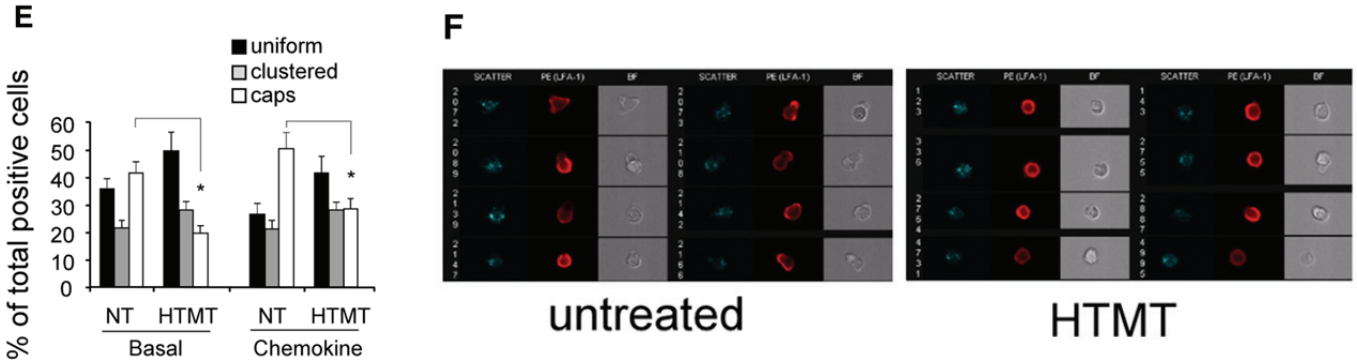

"We observed that the H1R agonist HTMT reduced LFA-1 distribution significantly in clusters and caps (big polar patches) on activated T cells (Fig. 4), an event that facilitates cell– cell contacts and adhesive interactions, which are required for efficient migration through the endothelium [36]. Integrin distribution in clusters indicates increased lateral mobility and higher binding avidity [35, 36], and it has been shown recently that integrin clusters are associated with integrin-increased affinity, further emphasizing the importance of adhesion molecule distribution on cell surface [43]."

Reference: Lapilla, M., B. Gallo, M. Martinello, C. Procaccini, M. Costanza, S. Musio, B. Rossi, S. Angiari*, et al.*, *Histamine regulates autoreactive T cell activation and adhesiveness in inflamed brain microcirculation.* J Leukoc Biol, 2011. **89**(2): 259-67.

~ ~ ~ ~ ~ ~

Preferential pDC-MDCC conjugate formation and transfer of cellular components with HSV infection

Summary: Analysis of the interaction of plasmacytoid dendritic cells (pDC) and monocyte-derived dendritic cells (MDDC) by imageStream cytometry combines the statistical robustness of the flow cytometer with the imaging sensitivity of microscopy. We observed that BDCA+ pDC (orange) preferentially formed conjugates (red gate) with the HSV-infected (B) vs. uninfected (A) CFSE+ MDDC (green) and preferentially took-up cellular components from the infected vs. the uninfected cells, as indicated by the increased percentage of single pDC (R3) with internalized CFSE.

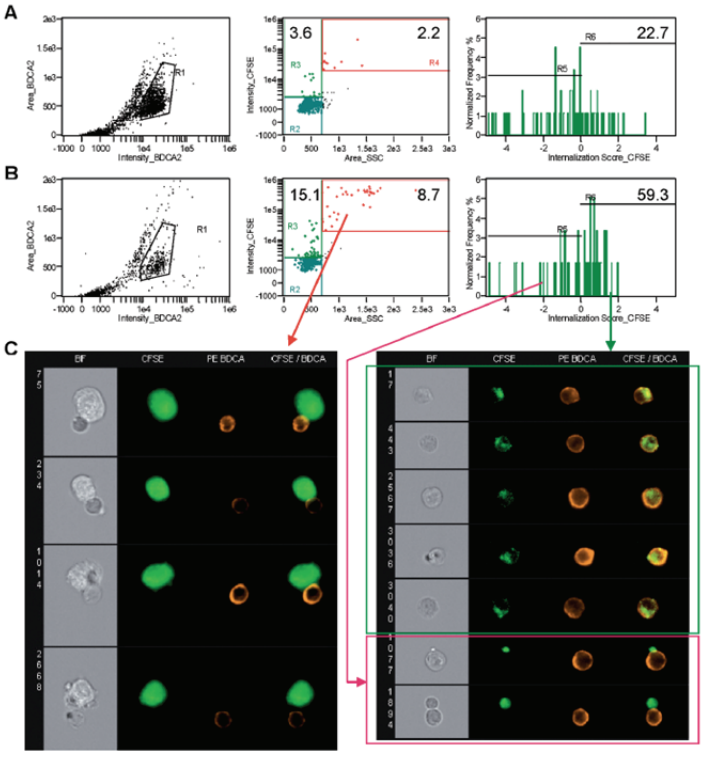

"In this study, we have evaluated the interaction of HSV-infected MDDC with pDC using a combination of traditional flow cytometric and imaging flow cytometric techniques. We report here that MDDC infected with HSV are able to stimulate IFN-α and chemokine production by pDC. Additionally, we demonstrate the preferential transfer of cellular components from HSVinfected MDDC vs. uninfected MDDC to pDC. Together, these results indicate that heterogeneous populations of DC interact to generate an effective IFN-α response."

Reference: Megjugorac, N.J., E.S. Jacobs, A.G. Izaguirre, T.C. George, G. Gupta, and P. Fitzgerald-Bocarsly, *Image-based study of interferongenic interactions between plasmacytoid dendritic cells and HSV-infected monocyte-derived dendritic cells.* Immunol Invest, 2007. **36**(5-6): 739-61.

Expression and maintenance of KHSV infection in tonsillar B cells

Summary: This ImageStream assay quantifies the expression and maintenance of Kaposi sarcoma–associated herpesvirus (KHSV) within human tonsillar B cells. KHSV-infected cells are identified as those events with latency-associated nuclear antigen (LANA) spots (A). Isolated B cells cultured in the presence of KHSV for 2-3 days (B) or for a 7day time course (C) demonstrate preferential growth of KHSV+ B cells. The ImageStream was further used to show that the cells expressing the λ-light chain of the B cell receptor were predominantly responsible for the observed maintenance of KHSV infection.

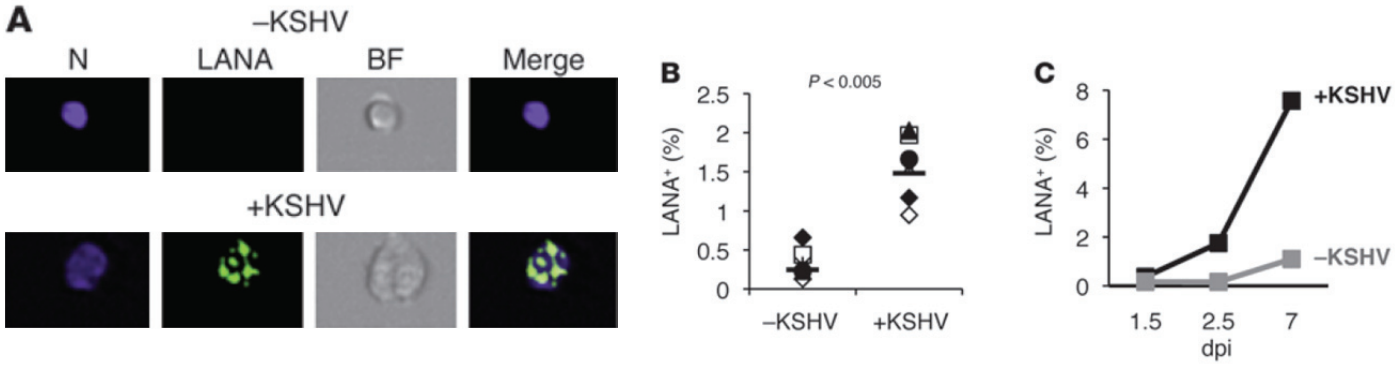

"To identify the cell type that potentially represents both the initial target of KSHV infection and the cell of origin for at least multicentric Castleman disease (MCD) and possibly primary effusion lymphoma (PEL), we exposed primary human tonsillar B cells to purified KSHV and characterized the cells that became latently infected using multispectral imaging flow cytometry (MIFC), a high-throughput single-cell imaging technique."

Reference: Hassman, L.M., T.J. Ellison, and D.H. Kedes, *KSHV infects a subset of human tonsillar B cells, driving proliferation and plasmablast differentiation.* J Clin Invest, 2010. **121**(2): 752-68.

~ ~ ~ ~ ~ ~

HIV-induced nuclear translocation of IRF3

Summary: This ImageStream assay measures IRF3 nuclear localization (by quantifying the similarity between the IRF3 and nuclear images on a per-cell basis) in 293T cells after co-culturing with MT4C5 cells. The ImageStream's unique ability to objectively measure translocation for thousands of cells per sample allows statistically robust discrimination of the samples, which is of critical importance given their heterogeneous response characteristics.

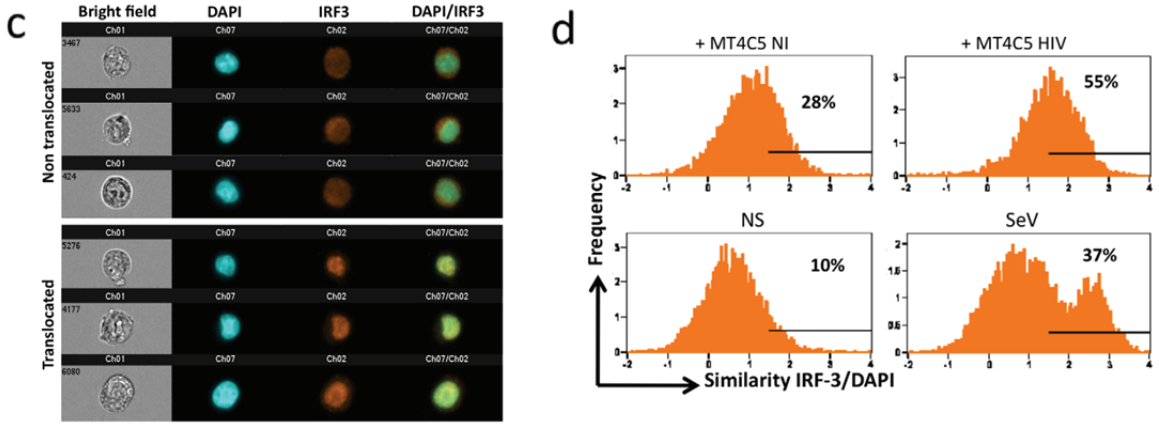

"A quantitative analysis based on the similarity of IRF3 and DAPI stainings revealed a 2-fold increase when 293T-4X4 were incubated with HIV-infected cells (55% vs 28% for cocultures of HIV-infected and non infected MT4C5 cells, respectively, Fig. 5d). As expected, with SeV, there was a 3-4-fold increase in the similarity score. Therefore, contact with HIV-infected cells induces nuclear translocation of IRF3 in 293T-4X4 cells."

Reference: Lepelley, A., S. Louis, M. Sourisseau, H.K. Law, J. Pothlichet, C. Schilte, L. Chaperot, J. Plumas*, et al.*, *Innate Sensing of HIV-Infected Cells.* PLoS Pathog, 2011. **7**(2): e1001284.

Measurement of TLR-mediated NF-κB nuclear translocation in whole blood pDC

Summary: This ImageStream assay measures NF-κB (pink) nuclear localization (by quantifying the similarity between the NF-κB and nuclear images on a per-cell basis) in CD123+BDCA-2+ pDC after incubation with the TLR-7 agonist R848. Median Similarity scores of pDC from whole blood samples incubated with the indicated dose of R848 for 60 minutes (bottom) or incubated for the indicated time with 1 μg/mL R848 (top) are plotted at right. Measuring nuclear translocation within non-enriched pDC, which account for ~0.1% of whole blood leukocytes, requires rapid imaging in order to obtain statistically relevant numbers of pDC for the translocation analysis.

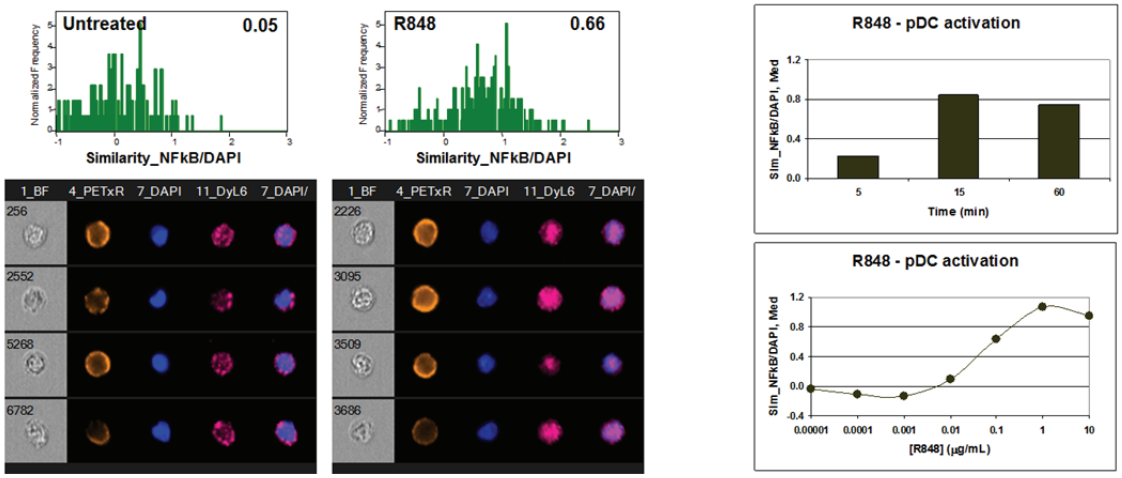

"Here we use imaging flow cytometry to quantify nuclear localization of NFkB in monocytes and pDC directly in whole blood samples. We show that very low doses (100 pg/mL) of LPS and TNF-a activate monocyte NFkB translocation within 5 minutes. We also show dose and time kinetics of TLR7 agonist R848-induced NFkB translocation of pDC directly in whole blood. These data demonstrate image-based measurement of nuclear translocation within rare cell and virus-specific innate immune cells using ImageStream technology."

Reference: T.C. George, B.E. Hall, S.M. Mordecai, S.L. Friend, and R. Kong, *Measurement of rare innate immune cell activation directly in whole blood using imaging flow cytometry.* Poster presentation AAI 2010.

~ ~ ~ ~ ~ ~

Internalization of exosomes by monocytes

Summary: This ImageStream assay quantifies the binding and internalization of breat milk-derived exosomes by human monocytes. The ImageStream's high speed imaging capacity enabled analysis of 10,000 events per sample for robust statistics. The internalization feature measures the relative amount of total exosome probe (green) that falls inside the CD14 ring stain (red).

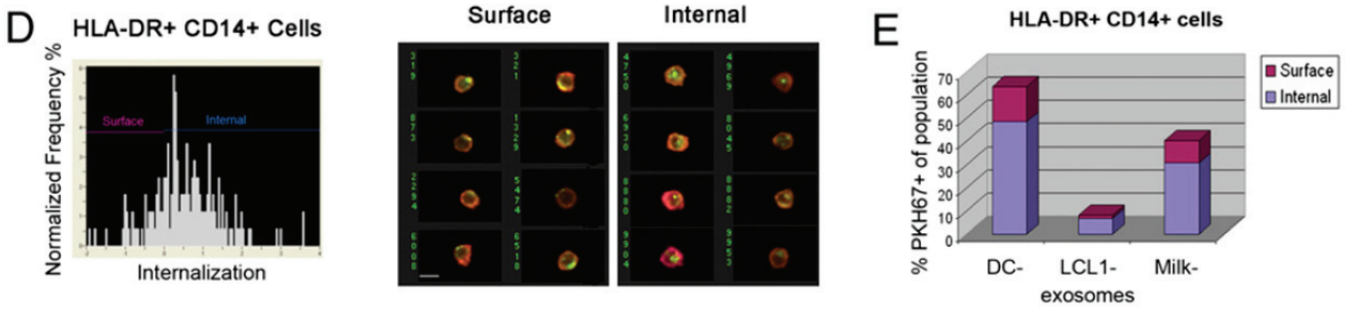

"In conclusion, we showed that exosomes, found in breast milk and produced by human monocyte-derived DCs and an EBV2 Bcell line, do not preferably associate with B cells. Instead, they mainly target monocytes, which actively engulf exosomes, as demonstrated for milk and DC exosomes."

Reference: Vallhov, H., C. Gutzeit, S.M. Johansson, N. Nagy, M. Paul, Q. Li, S. Friend, T.C. George*, et al.*, *Exosomes containing glycoprotein 350 released by EBV-transformed B cells selectively target B cells through CD21 and block EBV infection in vitro.* J Immunol, 2010. **186**(1): 73-82.

Merocytosis of irradiated β-islet cell fragments by mcDCs

Summary: This ImageStream assay quantifies the uptake of CFSE-labeled (green) β-islet cell material by CD11b+ DC and mcDCs. Representative images of CD11b+ DC and merocytic dendritic cells (mcDC) are shown in (A) and (B). Automated counting of islet-derived CFSE particles within each DC was done specifically within the DC cytoplasmic mask. The number of CFSE particles per DC is shown in (C), while the mean particle number and intensity per DC is shown in (D) and (E), respectively.

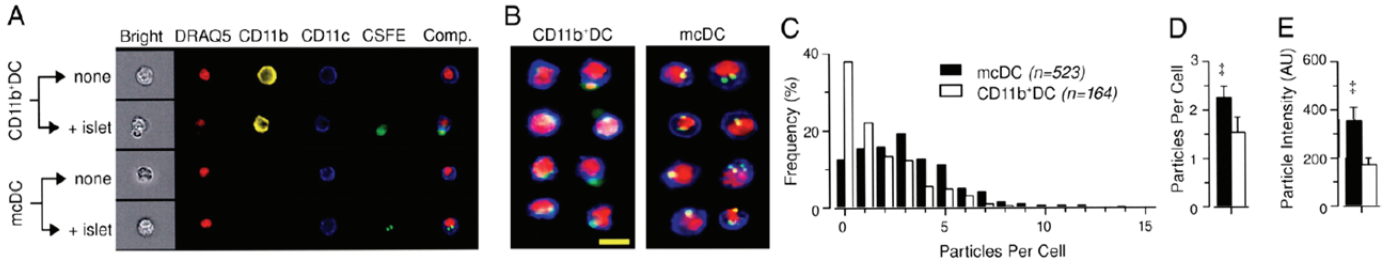

"Note that the CD11b+ DCs incubated with irradiated, CFSE-labeled islet cells exhibited diffuse CFSE staining within the cytoplasm, typical of phagocytosis and catabolism of ingested cells, whereas the corresponding mcDCs contained cells with distinct punctate vesicles containing CFSE. This is more easily seen in the composite image galleries shown in Fig. 2B. In this study, several of the CD11b+ DCs have not only widely distributed CFSE staining but also cytoplasm-localized apoptotic bodies (DRAQ-5+), consistent with macropinocytosis. In contrast, the mcDCs exhibit multiple merocytic vesicles of moderate to high intensity for CFSE."

Reference: Katz, J.D., J.K. Ondr, R.J. Opoka, Z. Garcia, and E.M. Janssen, *Cutting Edge: Merocytic Dendritic Cells Break T Cell Tolerance to {beta} Cell Antigens in Nonobese Diabetic Mouse Diabetes.* J Immunol, 2010. **185**(4): 1999-2003.

Related reference from the same group – reboulet 2010 - Reboulet, R.A., C.M. Hennies, Z. Garcia, S. Nierkens, and E.M. Janssen, *Prolonged antigen storage endows merocytic dendritic cells with enhanced capacity to prime anti-tumor responses in tumor-bearing mice.* J Immunol, 2010. **185**(6): 3337-47.

c-Myc-induced apoptosis of terminally differentiating B cells

Summary: This ImageStream assay quantifies apoptosis using the morphology of the nuclear image. Cells with fragmented (increased nuclear texture, Spot Small Total) were gated to determine the apoptotic percentage of plasma cells, plasma precursors, and B cells from control or c-Myc+/+ mice, with representative cells shown at right.

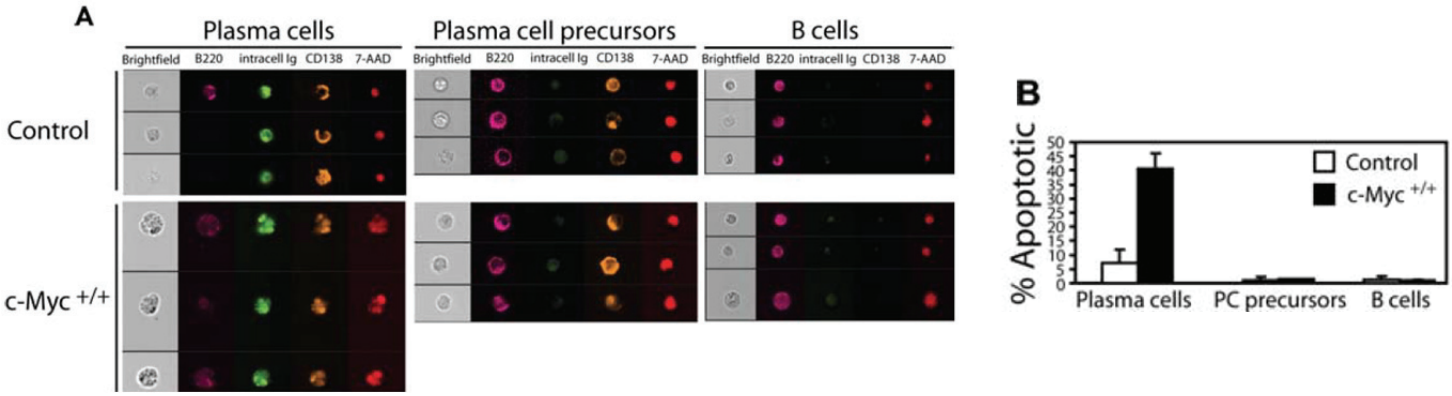

"In this study, we show that targeting *Myc* to the *Igh* Cα locus in mice impairs both primary and secondary humoral immune responses by failing to generate mature Ab-secreting PCs to TI and TD Ags….As such, tumor progression is curbed by c-Myc- induced apoptosis of mature longlived effector B cells unless apoptotic pathways such as members of the Bcl-2 family are concomitantly disabled."

Reference: Khuda, S.E., W.M. Loo, S. Janz, B. Van Ness, and L.D. Erickson, *Deregulation of c-Myc Confers distinct survival requirements for memory B cells, plasma cells, and their progenitors.* J Immunol, 2008. **181**(11): 7537-49.

Reference list – Immuology applications for the ImageStream

Ackerman, M.E., B. Moldt, R.T. Wyatt, A.S. Dugast, E. McAndrew, S. Tsoukas, S. Jost, C.T. Berger*, et al.*, *A robust, high-throughput assay to determine the phagocytic activity of clinical antibody samples.* J Immunol Methods, 2010. **366**(1-2): 8-19.

Ahmed, F., S. Friend, T.C. George, N. Barteneva, and J. Lieberman, *Numbers matter: quantitative and dynamic analysis of the formation of an immunological synapse using imaging flow cytometry.* J Immunol Methods, 2009. **347**(1-2): 79-86.

Beinborn, M., A. Blum, L. Hang, T. Setiawan, J.C. Schroeder, K. Stoyanoff, J. Leung, and J.V. Weinstock, *TGF-beta regulates T-cell neurokinin-1 receptor internalization and function.* Proc Natl Acad Sci U S A, 2010. **107**(9): 4293-8.

Beum, P.V., M.A. Lindorfer, B.E. Hall, T.C. George, K. Frost, P.J. Morrissey, and R.P. Taylor, *Quantitative analysis of protein co-localization on B cells opsonized with rituximab and complement using the ImageStream multispectral imaging flow cytometer.* J Immunol Methods, 2006. **317**(1-2): 90-9.

Beum, P.V., D.A. Mack, A.W. Pawluczkowycz, M.A. Lindorfer, and R.P. Taylor, *Binding of rituximab, trastuzumab, cetuximab, or mAb T101 to cancer cells promotes trogocytosis mediated by THP-1 cells and monocytes.* J Immunol, 2008. **181**(11): 8120-32.

Burbach, B.J., R. Srivastava, R.B. Medeiros, W.E. O'Gorman, E.J. Peterson, and Y. Shimizu, *Distinct regulation of integrin-dependent T cell conjugate formation and NF-kappa B activation by the adapter protein ADAP.* J Immunol, 2008. **181**(7): 4840-51.

Buss, S.N., S. Hamano, A. Vidrich, C. Evans, Y. Zhang, O.R. Crasta, B.W. Sobral, C.A. Gilchrist*, et al.*, *Members of the Entamoeba histolytica transmembrane kinase family play non-redundant roles in growth and phagocytosis.* International Journal for Parasitology, 2010. **In Press, Corrected Proof**.

Calzada-Nova, G., W.M. Schnitzlein, R.J. Husmann, and F.A. Zuckermann, *North American porcine reproductive and respiratory syndrome viruses inhibit type I interferon production by plasmacytoid dendritic cells.* J Virol, 2011. **85**(6): 2703-13.

Chang, S., K. Kodys, and G. Szabo, *Impaired expression and function of toll-like receptor 7 in hepatitis C virus infection in human hepatoma cells.* Hepatology, 2010. **51**(1): 35-42.

Collins, C.B., J. Ho, T.E. Wilson, J.D. Wermers, J.L. Tlaxca, M.B. Lawrence, M. Solga, J. Lannigan*, et al.*, *CD44 deficiency attenuates chronic murine ileitis.* Gastroenterology, 2008. **135**(6): 1993-2002.

Danis, B., T.C. George, S. Goriely, B. Dutta, J. Renneson, L. Gatto, P. Fitzgerald-Bocarsly, A. Marchant*, et al.*, *Interferon regulatory factor 7-mediated responses are defective in cord blood plasmacytoid dendritic cells.* Eur J Immunol, 2008. **38**(2): 507-17.

De Rose, R., A.N. Zelikin, A.P.R. Johnston, A. Sexton, S.-F. Chong, C. Cortez, W. Mulholland, F. Caruso*, et al.*, *Binding, Internalization, and Antigen Presentation of Vaccine-Loaded Nanoengineered Capsules in Blood.* Advanced Materials, 2008. **20**(24): 4698-4703.

Decaluwe, H., M. Taillardet, E. Corcuff, I. Munitic, H.K. Law, B. Rocha, Y. Riviere, and J.P. Di Santo, *{gamma}c deficiency precludes CD8+ T cell memory despite formation of potent T cell effectors.* Proc Natl Acad Sci U S A, 2010.

Elishmereni, M., H.T. Alenius, P. Bradding, S. Mizrahi, A. Shikotra, Y. Minai-Fleminger, D. Mankuta, R. Eliashar*, et al.*, *Physical interactions between mast cells and eosinophils: a novel mechanism enhancing eosinophil survival in vitro.* Allergy, 2010. **66**(3): 376-85.

Fanning, S.L., T.C. George, D. Feng, S.B. Feldman, N.J. Megjugorac, A.G. Izaguirre, and P. Fitzgerald-Bocarsly, *Receptor cross-linking on human plasmacytoid dendritic cells leads to the regulation of IFN-alpha production.* J Immunol, 2006. **177**(9): 5829-39.

George, T.C., S.L. Fanning, P. Fitzgeral-Bocarsly, R.B. Medeiros, S. Highfill, Y. Shimizu, B.E. Hall, K. Frost*, et al.*, *Quantitative measurement of nuclear translocation events using similarity analysis of multispectral cellular images obtained in flow.* J Immunol Methods, 2006. **311**(1-2): 117-29.

Hassman, L.M., T.J. Ellison, and D.H. Kedes, *KSHV infects a subset of human tonsillar B cells, driving proliferation and plasmablast differentiation.* J Clin Invest, 2010. **121**(2): 752-68.

Hochweller, K., G.H. Wabnitz, Y. Samstag, J. Suffner, G.J. Hammerling, and N. Garbi, *Dendritic cells control T cell tonic signaling required for responsiveness to foreign antigen.* Proc Natl Acad Sci U S A, 2010. **107**(13): 5931-6.

Hoffmann, S., B.H. Hosseini, M. Hecker, I. Louban, N. Bulbuc, N. Garbi, G.H. Wabnitz, Y. Samstag*, et al.*, *Single cell force spectroscopy of T cells recognizing a myelin-derived peptide on antigen presenting cells.* Immunol Lett, 2011. **136**(1): 13-20.

Hosseini, B.H., I. Louban, D. Djandji, G.H. Wabnitz, J. Deeg, N. Bulbuc, Y. Samstag, M. Gunzer, *et al.*, *Immune synapse formation determines interaction forces between T cells and antigen-presenting cells measured by atomic force microscopy.* Proc Natl Acad Sci U S A, 2009. **106**(42): 17852-7.

Iype, T., M. Sankarshanan, I.S. Mauldin, D.W. Mullins, and U. Lorenz, *The protein tyrosine phosphatase SHP-1 modulates the suppressive activity of regulatory T cells.* J Immunol, 2010. **185**(10): 6115-27.

Katz, J.D., J.K. Ondr, R.J. Opoka, Z. Garcia, and E.M. Janssen, *Cutting Edge: Merocytic Dendritic Cells Break T Cell Tolerance to {beta} Cell Antigens in Nonobese Diabetic Mouse Diabetes.* J Immunol, 2010. **185**(4): 1999-2003.

Khuda, S.E., W.M. Loo, S. Janz, B. Van Ness, and L.D. Erickson, *Deregulation of c-Myc Confers distinct survival requirements for memory B cells, plasma cells, and their progenitors.* J Immunol, 2008. **181**(11): 7537-49.

Lapilla, M., B. Gallo, M. Martinello, C. Procaccini, M. Costanza, S. Musio, B. Rossi, S. Angiari, *et al.*, *Histamine regulates autoreactive T cell activation and adhesiveness in inflamed brain microcirculation.* J Leukoc Biol, 2011. **89**(2): 259-67.

Lee, H.K., J.M. Lund, B. Ramanathan, N. Mizushima, and A. Iwasaki, *Autophagy-dependent viral recognition by plasmacytoid dendritic cells.* Science, 2007. **315**(5817): 1398-401.

Lepelley, A., S. Louis, M. Sourisseau, H.K. Law, J. Pothlichet, C. Schilte, L. Chaperot, J. Plumas, *et al.*, *Innate Sensing of HIV-Infected Cells.* PLoS Pathog, 2011. **7**(2): e1001284.

Matsuda, J.L., T.C. George, J. Hagman, and L. Gapin, *Temporal dissection of T-bet functions.* J Immunol, 2007. **178**(6): 3457-65.

Megjugorac, N.J., E.S. Jacobs, A.G. Izaguirre, T.C. George, G. Gupta, and P. Fitzgerald-Bocarsly, *Image-based study of interferongenic interactions between plasmacytoid dendritic cells and HSV-infected monocyte-derived dendritic cells.* Immunol Invest, 2007. **36**(5-6): 739-61.

Pawluczkowycz, A.W., F.J. Beurskens, P.V. Beum, M.A. Lindorfer, J.G. van de Winkel, P.W. Parren, and R.P. Taylor, *Binding of submaximal C1q promotes complement-dependent cytotoxicity (CDC) of B cells opsonized with anti-CD20 mAbs ofatumumab (OFA) or rituximab (RTX): considerably higher levels of CDC are induced by OFA than by RTX.* J Immunol, 2009. **183**(1): 749-58.

Petrovas, C., B. Chaon, D.R. Ambrozak, D.A. Price, J.J. Melenhorst, B.J. Hill, C. Geldmacher, J.P. Casazza, *et al.*, *Differential association of programmed death-1 and CD57 with ex vivo survival of CD8+ T cells in HIV infection.* J Immunol, 2009. **183**(2): 1120-32.

Ramos, H.J., A.M. Davis, T.C. George, and J.D. Farrar, *IFN-alpha is not sufficient to drive Th1 development due to lack of stable T-bet expression.* J Immunol, 2007. **179**(6): 3792-803.

Reboulet, R.A., C.M. Hennies, Z. Garcia, S. Nierkens, and E.M. Janssen, *Prolonged antigen storage endows merocytic dendritic cells with enhanced capacity to prime anti-tumor responses in tumor-bearing mice.* J Immunol, 2010. **185**(6): 3337-47.

Sancho, D., O.P. Joffre, A.M. Keller, N.C. Rogers, D. Martinez, P. Hernanz-Falcon, I. Rosewell, and C. Reis e Sousa, *Identification of a dendritic cell receptor that couples sensing of necrosis to immunity.* Nature, 2009. **458**(7240): 899-903.

Santer, D.M., B.E. Hall, T.C. George, S. Tangsombatvisit, C.L. Liu, P.D. Arkwright, and K.B. Elkon, *C1q deficiency leads to the defective suppression of IFN-alpha in response to nucleoprotein containing immune complexes.* J Immunol, 2010. **185**(8): 4738-49.

Tibrewal, N., Y. Wu, V. D'Mello, R. Akakura, T.C. George, B. Varnum, and R.B. Birge, *Autophosphorylation docking site Tyr-867 in Mer receptor tyrosine kinase allows for dissociation of multiple signaling pathways for phagocytosis of apoptotic cells and down-modulation of lipopolysaccharide-inducible NF-kappaB transcriptional activation.* J Biol Chem, 2008. **283**(6): 3618-27.

Vallhov, H., C. Gutzeit, S.M. Johansson, N. Nagy, M. Paul, Q. Li, S. Friend, T.C. George, *et al.*, *Exosomes containing glycoprotein 350 released by EBV-transformed B cells selectively target B cells through CD21 and block EBV infection in vitro.* J Immunol, 2010. **186**(1): 73-82.

Vujanovic, L., D.E. Szymkowski, S. Alber, S.C. Watkins, N.L. Vujanovic, and L.H. Butterfield, *Virally infected and matured human dendritic cells activate natural killer cells via cooperative activity of plasma membrane-bound TNF and IL-15.* Blood, 2010. **116**(4): 575-83.

Wang, H., B. Grzywacz, D. Sukovich, V. McCullar, Q. Cao, A.B. Lee, B.R. Blazar, D.N. Cornfield, *et al.*, *The unexpected effect of cyclosporin A on CD56+CD16- and CD56+CD16+ natural killer cell subpopulations.* Blood, 2007. **110**(5): 1530-9.

Xu, C., A. Lo, A. Yammanuru, A.S. Tallarico, K. Brady, A. Murakami, N. Barteneva, Q. Zhu*, et al.*, *Unique biological properties of catalytic domain directed human anti-CAIX antibodies discovered through phage-display technology.* PLoS One, 2010. **5**(3): e9625.